

uSF: Learning Neural Semantic Field with Uncertainty

V.S. Skorokhodov¹, D.M. Drozdova¹, D.A. Yudin^{1,2,3*}

¹Moscow Institute of Physics and Technology, Moscow, Russia

²AIRI (Artificial Intelligence Research Institute), Moscow, Russia

³Federal Research Center “Computer Science and Control”, Moscow, Russia

*e-mail: yudin.da@mipt.ru

Abstract. Recently, there has been an increased interest in NeRF methods which reconstruct differentiable representation of three-dimensional scenes. One of the main limitations of such methods is their inability to assess the confidence of the model in its predictions. In this paper, we propose a new neural network model for the formation of extended vector representations, called uSF, which allows the model to predict not only color and semantic label of each point, but also estimate the corresponding values of uncertainty. We show that with a small number of images available for training, a model that quantifies uncertainty performs better than a model without such functionality. Code of the uSF approach is publicly available at <https://github.com/sevashasla/usf/>.

Keywords: Neural semantic field, Neural network, Learning, Uncertainty, 3D scene

1 Introduction

Over the past few years, many researchers have focused on the development of the field of differentiable scene representation. This development began with the appearance of the first NeRF method [1], which demonstrated the photo-realistic quality of novel views generation. Various modifications of the original method allow us to additionally solve such problems as depth estimation [2], semantic segmentation [3,4], object detection [5]. Among the disadvantages of the NeRF methods one can note high computational complexity [6,7], the need for a large number of images [8,9] in the training dataset and the inability to estimate the confidence of the model in its predictions. Quantifying uncertainty is a crucial aspect for minimizing possible risks for tasks in various fields, for example robotics [10] and autonomous driving [11,12].

As shown in Fig. 1 we propose a novel NeRF-based method that reconstructs the neural radiance and the neural semantic fields. The previously proposed NeRF methods only considered estimating the uncertainty for color predictions, i.e. regression task [13–15]. Our method additionally introduces the possibility of quantifying uncertainty for predicted semantic labels, i.e. classification task. There are two types of uncertainty: aleatoric and epistemic. Aleatoric uncertainty reflects the noise inherent in the input data. Epistemic uncertainty reflects what the model does not know due to a lack of data, too simple architecture, or inefficient training process. In both cases, aleatoric uncertainty is estimated. The high value of uncertainty may also indicate errors occurred in the data preparation process, for example, poor quality of labelling in segmentation tasks. We choose aleatoric uncertainty over epistemic uncertainty because quantifying aleatoric uncertainty does not require major changes in network architecture and multiple inferences or training. Adding uncertainty estimation to the algorithm pipeline does not degrade the quality of reconstruction with a sufficient number of images and improves the quality with a small training dataset. Our method is also computationally efficient because it uses trainable positional encoding based on hashing [6]. We summarize our main contributions as follows:

- We have proposed a new neural network model called uSF, which allows to add the ability to quantify the uncertainty for predicted neural semantic field, while maintaining quantifying uncertainty for neural radiance field.
- Due to the use of trainable positional encoding based on hashing, our approach is able to noticeably reduce the running time of the algorithm.

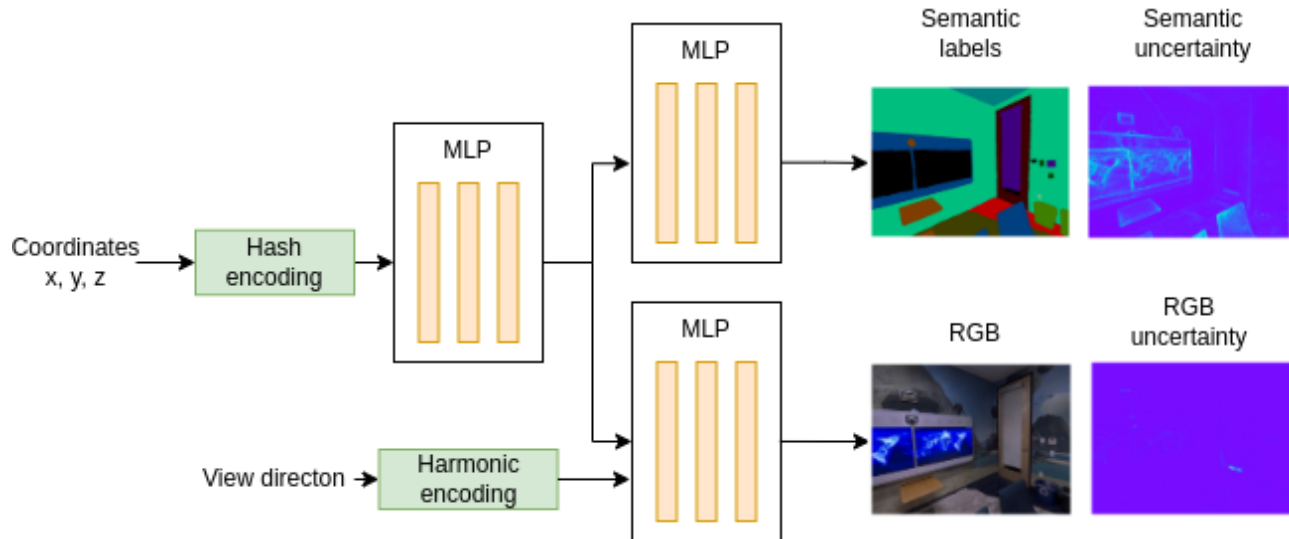


FIG. 1. We propose the model named uSF to predict both color and semantic labels and estimate corresponding uncertainty.

- We have shown that quantifying uncertainty for both color and semantic labels predictions improves the quality of semantic 3D-scene reconstruction with a small number of images in the training set from open Replica Dataset.

2 Related Work

2.1 Neural Radiance Fields

Due to the great popularity of the NeRF method, the researchers have developed a large number of works expanding the possibilities of the original method. Some papers address the inefficiency of training and rendering [6, 7, 16, 17]. The other methods make it possible to apply the NeRF under certain restrictions: limited number of images in the training dataset [8, 9, 18, 19], lack of information about camera poses [20], unlimited scene space [21], dynamic scenes [22, 23].

2.2 Neural Semantic Fields

There are NeRF methods that can predict not only the color at each point of the scene, but also corresponding semantic labels. The Semantic-NeRF [3] method reconstructs the neural semantic field with the help of an additional head in the model architecture. The process of getting semantic labels at a point is similar to getting a color. This method is highly robust to the presence of outliers in the training data, yielding quality results even with 90% noise.

Another approach to segmentation is shown in the NeRF-SOS [24] method. The work successfully combines self-supervised 2D visual features for 3D semantic segmentation. Separate head outputs for segmentation are trained similar to Dino-ViT [25]. NeSF [26] is the method that produces generalizable neural semantic fields. The authors propose to firstly recover 3D density fields upon which 3D semantic segmentation model is trained supervised by posed 2D semantic maps. The pre-trained NeRF model is used to sample the volumetric density grid for further conversion into a semantic-feature grid. Semantic Ray [4] also has generalization ability and uses Cross-Reprojection Attention module to obtain such result.

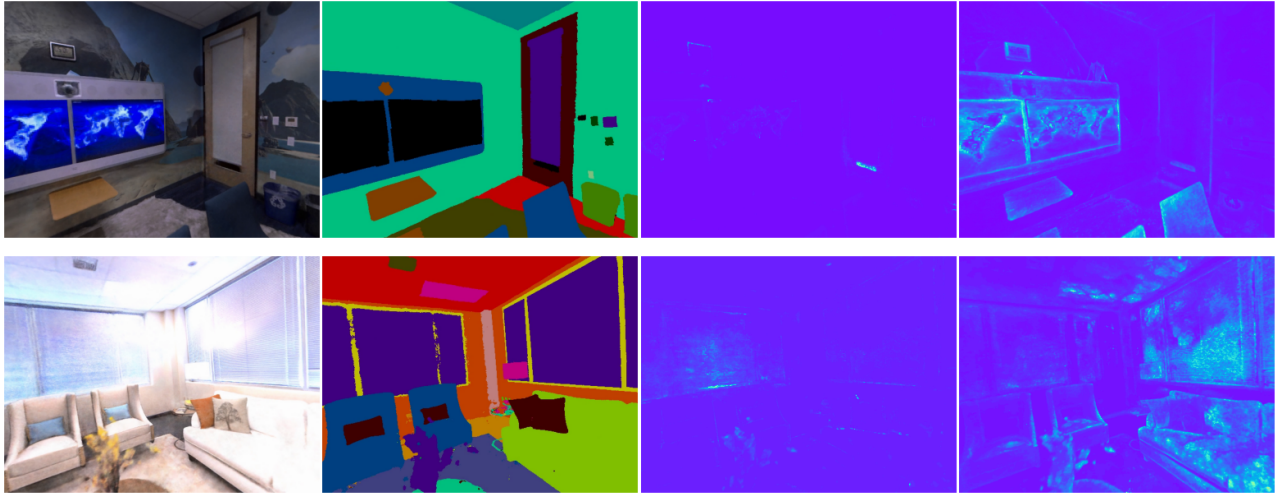


FIG. 2. From left to right we show the predicted color, predicted semantic labels, rgb uncertainty and semantic uncertainty during training process.

2.3 Uncertainty Estimation

To estimate the aleatoric uncertainty, a probability distribution is imposed on the outputs of the model. This approach assumes that there is noise in the input data, the distribution parameters of which can be predicted as some function of the data. To predict epistemic uncertainty, it is a common practice to impose a distribution on the model parameters (Bayesian neural networks (BNN) [27–29]). The disadvantage of these methods for quantifying epistemic uncertainty is the requirement to train the model several times and make multiple inferences. There are also approaches that simultaneously estimate both types of uncertainties [30–32].

Uncertainty quantification in various implementations has already been applied in several NeRF models. The Active NeRF [8] is designed to deal with the limited number of images in the training set. In this method, the estimated aleatoric uncertainty is used for adding new frames to the training data during the iterations of active learning. In the NeRF-W [13] method aleatoric uncertainty is used to identify non-static objects that should be removed from the prediction. This approach allows you to obtain the scene reconstruction consisting only of static objects. The two following methods focus on quantifying of epistemic uncertainty. In the S-NeRF [14] method, it is assumed that all possible neural radiance fields for the scene are distributed according to a prior distribution, on the basis of which and the input data the model predicts a posterior distribution, with which the uncertainty is estimated. The CF-NeRF [15] method works similarly, but does not impose any preliminary restrictions on the distribution. Recently in Bayes’ Rays work [33] the authors have proposed a new method to estimate epistemic uncertainty that does not require any changes during training process. All of these methods try to quantify uncertainty for color or depth predictions, while in this paper we propose the approach for estimating corresponding uncertainty for semantic label predictions.

3 Methodology

3.1 Neural Network Model

The architecture of our model is MLP with ReLU activation functions and a hidden state dimension equal to 64 as shown in the Fig. 3. Similar to Active NeRF [8] and NeRF-W [13] pipeline we add an additional head to predict the color variance β_{rgb} which we use as rgb uncertainty. In our work we assume that it depends on the view direction.

We add two heads for semantic segmentation task. One outputs mean values (sem_1, \dots, sem_n) ,

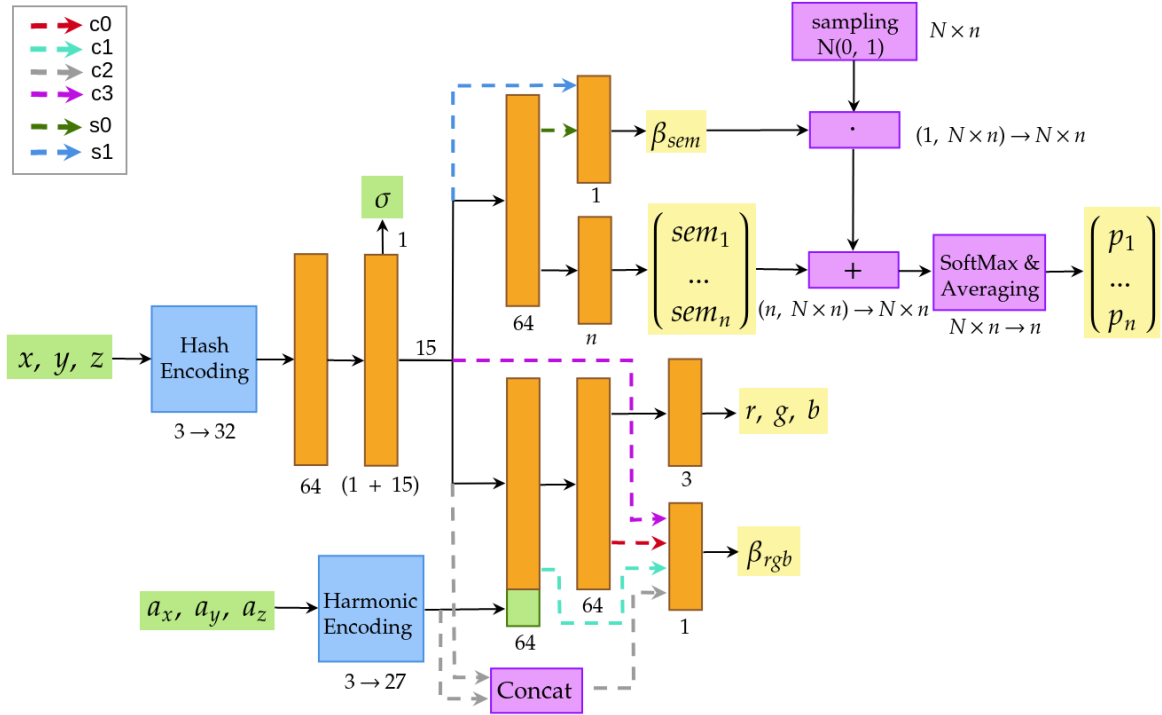


FIG. 3. uSF architecture. Orange rectangles are Linear + ReLU layers. Yellow rectangles are outputs of our model. We study different variants of our architecture in terms of the color (c0-c3) and the semantic (s0-s1) branches.

and the other predicts the variance β_{sem}^2 . We consider outputs of semantic heads to depend only on coordinates of the point, but not on view direction.

For semantic head we make MLP smaller than for color head with only two layers. We also use ReLU activation function and set the dimensionality of the hidden state to 64.

3.2 Uncertainty for Neural Radiance Field

As described in the previous section the color part of the architecture consists of two heads [32]. One outputs the mean value parameter of some normal distribution which we consider as the color at the point. The other head outputs the variance which depends both on the coordinates of the point and on the view direction corresponding to it. To get the final value of uncertainty, the softplus activation function is used:

$$\bar{\beta}^2 = \beta_0^2 + \log(1 + \exp(\beta^2)). \quad (1)$$

The β_0 parameter is the minimum possible value of rgb uncertainty. To obtain the uncertainty values at each point of 3D space of the scene we use volume render procedure. The example of the predicted rgb uncertainty is shown in the Fig. 2

3.3 Uncertainty for Neural Semantic Field

From the semantic head our model outputs the mean values (sem_i) and the variance (β_{sem}) of semantic logits. We assume that $logit_i \sim \mathcal{N}(sem_i, \beta_{sem}^2)$. We want to use a CrossEntropy for the network optimization, but there are some difficulties of obtaining the exact class probabilities because

one can't calculate such mathematical expectation 2.

$$\hat{p}_i = \mathbb{E} \text{SoftMax}(\{\text{logit}_1, \dots, \text{logit}_n\})_i \quad (2)$$

In order to deal with such problem we use an approximation. We generate $N = 10$ sets of logits from the corresponding normal distributions, then count SoftMax separately for each set, and then average the obtained results 3:

$$p_{pred,i} \approx \frac{1}{N} \hat{p}_i \quad (3)$$

During calculation we use the "reparametrization trick". Let $\xi \sim \mathcal{N}(a, \sigma^2)$, and $\eta \sim \mathcal{N}(0, 1)$. Then $\xi \stackrel{d}{=} a + \sigma \cdot \eta$. Then to generate logits, we firstly generate random values from $\mathcal{N}(0, 1)$, and then convert them to the form we want by multiplying by the standard deviation (β_{sem}) and adding the mean (sem_i). The example of the predicted semantic uncertainty is shown in the Fig. 2

3.4 Learning Approach

To train our model we use the following loss function 4, which consists of three terms:

$$Loss = \omega L_{rgb} + \lambda L_{semantic} + (1 - \omega) L_{uncert}, \quad (4)$$

where:

$$L_{rgb} = \frac{1}{N} \sum_{i=1}^N (C(r_i) - rgb_i)^2, \quad (5)$$

where $C(r_i)$ is predicted color for ray r_i , rgb_i is ground truth color for ray r_i .

$$L_{semantic} = \text{CrossEntropy}(p_{pred}, semantic_{gt}), \quad (6)$$

where p_{pred} is a set of predicted probabilities of semantic classes, $semantic_{gt}$ is a set of ground truth semantic labels.

$$L_{uncert} = \frac{1}{N} \sum_{i=1}^N \left(\frac{\|C(r_i) - rgb_i\|^2}{2\beta_{rgb}(r_i)^2} + \frac{1}{2} \log \beta_{rgb}(r_i)^2 + \frac{\eta}{N_{si}} \sum_{j=1}^{N_{si}} \alpha(r_i(t_j)) \right), \quad (7)$$

where $C(r_i)$ is predicted color for ray r_i , rgb_i is ground truth color for ray r_i , $\beta_{rgb}(r_i)^2$ is predicted variance for color for ray r_i , N_{si} is number of points t_j sampled on ray r_j , $\alpha(r_i(t_j))$ is point weight from volume rendering procedure [1] for ray r_i in point t_j , η is a hyperparameter which controls the strength of regularization.

Parameters ω, λ are hyperparameters. We have decided to make the different terms L_{rgb} and L_{uncert} , because they are both responsible for learning to make color predictions. In our experiments we change only ω and λ , and set $\alpha = 10^{-3}$.

We use Adam optimizer with $lr = 0.003$, $\beta = (0.9, 0.99)$, $eps = 10^{-15}$. During training the learning rate (lr) is changed according to equation 8. This equation is based on the fact that at the beginning learning is unstable due to big modulus of the gradient. Also at the end learning rate should be smaller to obtain better results.

$$lr(i) = lr(0) \cdot 0.1^{\min(1, \frac{i}{N_i})} \cdot \min\left(1, 10^{-3} + \frac{i}{N_{wi}}\right), \quad (8)$$

where i is iteration index, N_i is total number of iterations, N_{wi} is number of warmup iterations.

We use an early stopping during training. We firstly calculate mean of last 3 LPIPS values on eval dataset and then if $|\text{current LPIPS} - \text{mean}(\text{last 3 LPIPS})| < 10^{-3}$ is two times in a row, the training process is stopped.

Network architecture	best λ	best ω	mIoU
uSF (c0, s0)	$7.25 \cdot 10^{-2}$	$1.49 \cdot 10^{-5}$	0.570
uSF (c1, s0)	$8.47 \cdot 10^{-2}$	$5.51 \cdot 10^{-5}$	0.536
uSF (c2, s0)	$6.01 \cdot 10^{-2}$	$28.95 \cdot 10^{-5}$	0.5272
uSF (c3, s0)	$7.89 \cdot 10^{-2}$	$2.13 \cdot 10^{-5}$	0.5102
uSF (c0, s1)	$5.67 \cdot 10^{-2}$	$1.45 \cdot 10^{-5}$	0.5579

TAB. 1. Hyperparameter values at which the best quality of reconstruction is achieved on a given architecture.

We use PSNR, SSIM, LPIPS as the main metrics for the quality of color prediction like in other popular articles on 3D reconstruction. We use mIoU and accuracy as the main metric to qualify semantics maps prediction.

4 Experiments

4.1 Hardware and Software Setup

We have performed experiments on NVIDIA GeForce 2080 Ti, NVIDIA GeForce 2080, NVIDIA GeForce 3060 graphics cards. The model takes about 6GB of video memory during training. According to our estimates, full training lasts approximately 4-5 hours for one scene.

4.2 Datasets and Environments

As the main dataset, we use Replica [34], which is a set of synthetic room and office scenes with corresponding semantic masks. It is the photorealistic indoor dataset [35], which is widely used for scene reconstruction and mapping tasks, intelligent agent navigation, etc.

We use a pre-processed dataset from the Semantic NeRF [3] method with image size of 640×480 . Each scene contains 900 images with different view directions. We have performed all our experiments on scenes "room_0 "room_1"and "office_0"since they represent a typical home and office environment. For the dataset we have 2 different splitting options:

- Small: 27 images for training, 112 - for validation, 225 - for test,
- Large: 562 images for training, 112 - for validation, 225 - for test.

4.3 Architecture Choice

There are several options of the architectures for our method which are shown in Fig. 3. The options differ in the different number of layers and the presence of dependence on the view direction. To properly select the optimal hyperparameters λ and ω , we firstly have manually found rough estimates for the optimum, and then used 10 runs of Bayesian hyperparameter fitting for each architecture. We have chosen the search interval for optimal hyperparameters: $\sim Uniform[10^{-5}, 10^{-3}]$ for ω and $\sim Uniform[10^{-3}, 10^{-1}]$ for λ .

During the search we use only one scene room_0 from Replica Dataset, because, as practice shows, the quality of reconstruction on it is slightly worse than on the rest of the scenes. We use only small (27) training set for all experiments.

As shown in Tab. 1 the best results are achieved with uSF (c0, s0). The experiments have also proved, that is it better to consider uncertainty β_{rgb} as dependent on the view direction.

Scene	mIoU	PSNR	SSIM	LPIPS	Accuracy	$T_{\text{render, s}}$	Encoding	Architecture
room_0	0.961	31.024	0.902	0.109	0.980	1.993	hash	Small
	0.749	22.538	0.667	0.562	0.823	0.893	freq	
	-	31.067	0.905	0.104	-	1.073	hash	
	-	22.486	0.666	0.567	-	1.011	freq	
office_0	0.982	39.493	0.975	0.030	0.992	2.583	hash	Small
	0.849	28.452	0.835	0.438	0.914	1.500	freq	
	-	39.958	0.979	0.022	-	1.557	hash	
	-	27.641	0.822	0.485	-	1.131	freq	
room_1	-	36.369	0.956	0.042	-	0.753	hash	Small
	-	33.179	0.896	0.164	-	10.300	freq	Large

TAB. 2. Influence of positional encoding and model size on the quality of reconstruction of 3D scenes from Replica dataset.

Training sample size	Metrics	uSF (w/o uncert.)	uSF (rgb uncert.)	uSF (semantic uncert.)	uSF (both uncert.)
Small	mIoU	0.587	0.549	0.604	0.598
	PSNR	22.171	22.192	22.989	22.931
Large	mIoU	0.975	0.975	0.977	0.977
	PSNR	34.757	34.760	34.979	34.936

TAB. 3. Average values of mIoU and PSNR metrics for different numbers of images in the training dataset in cases where the model doesn’t quantify uncertainty, estimates only rgb uncertainty, only semantic uncertainty, and both types of uncertainties.

4.4 Positional Encoding Choice

We aim to create an effective implementation of our method without deterioration in quality. To achieve this, we have used the hash positional encoding which is described in Instant-NGP [6] method. It allows us to significantly reduce the number of layers in the architecture and the size of dimensions. Hidden layer dimension is 64 instead of 256, number of dense layers is 5 instead of 8.

Additionally, we have performed experiments to compare the networks with different type of positional encoding and architectures. The model with efficient architecture using hash positional encoding has shown better results in terms of speed and quality than the model from the original NeRF [1] (8 dense layers, 1 skip-connection, hidden dimension is 256) using harmonic (frequency) positional encoding. The overall comparison results can be seen in Table 2.

4.5 Study of Different Uncertainties Usage in uSF Architecture

We have compared the recovery quality of neural radiance field and neural semantic field in cases where the model predicts only color and semantic labels, as well as when the model additionally estimates only RGB uncertainty, only semantic uncertainty and both types of uncertainty. The metric values are given in Table 3. The experiments have been carried out on different train datasets sizes: small with 27 images and large with 562 images.

As we can see, in the case where there are 27 images in the training set the average PSNR value increases slightly with the addition of the uncertainty estimation. The average mIoU value improves in the case of predicting only semantic uncertainty and both uncertainties. In the case of a large set, adding a prediction also has a positive effect on metric values. So adding an uncertainty estimation does not degrade the quality of the network’s predictions, and in some cases even improves it.

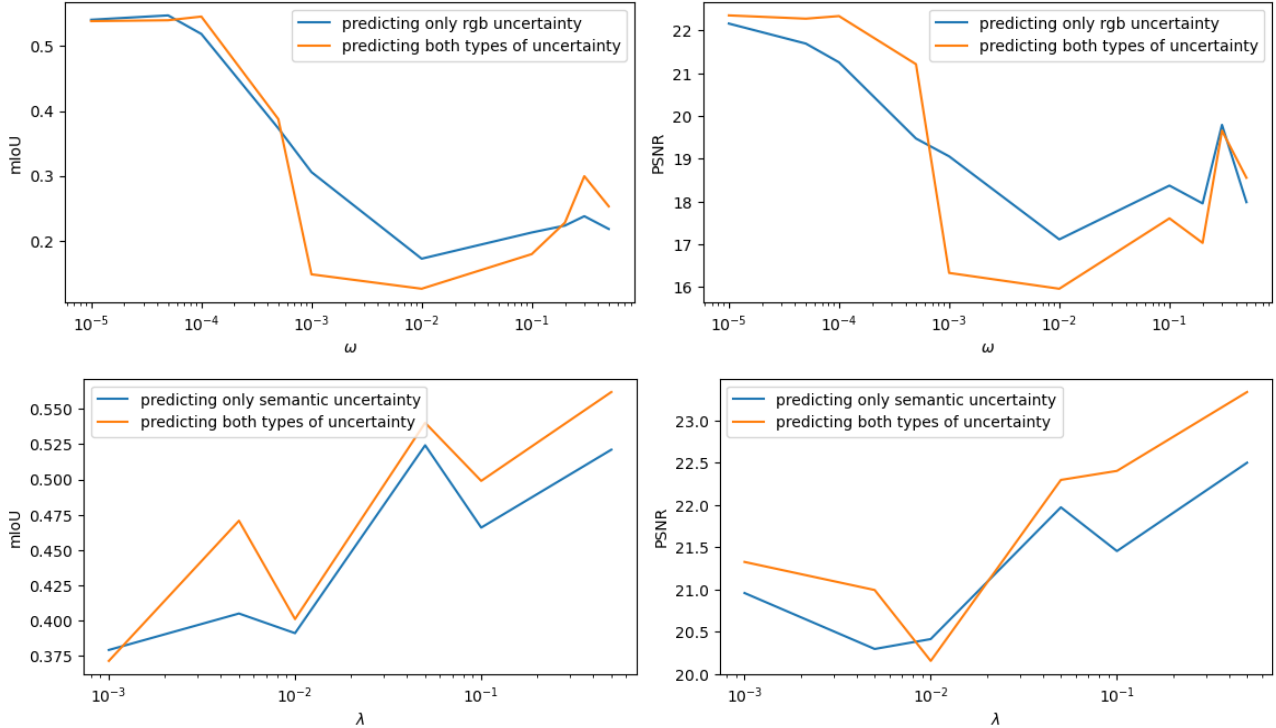


FIG. 4. The mean values of mIoU and PSNR depending on ω in the first row and λ in the second row for selected scenes from Replica Dataset.

4.6 Influence of the ω Hyperparameter on Semantic Field Reconstruction

We have performed experiments to see how the quality of recovery depends on the parameter ω . We fix $\lambda = 0.05$ and begin to change ω and carry out experiments on two different scenes that capture ordinary room and office environment. The small set of training images is used. At first, we predict only rgb uncertainty, after which we add prediction of semantic uncertainty.

The results are shown in the Fig. 4.

As we can see with increasing of the ω parameter the quality of both color and semantic labels reconstruction is decreasing. Also the dependencies of metrics on the ω parameters have two local maxima where the first is $\omega \approx 10^{-5}$, and the second is $\omega \approx 0.3$. In the first case metrics are better, so in the following our experiments we consider ω close to 10^{-5} .

4.7 Influence of the λ Hyperparameter on Semantic Field Reconstruction

A similar experiment with fixed ω has been performed for the parameter λ . The results are shown in the Fig. 4. As we can see with increasing of the λ parameter the quality of both color and semantic labels reconstruction is also increasing.

4.8 Quality of the Semantic 3D-Scene Reconstruction

We have compared the neural semantic fields reconstruction quality of our uSF method trained with the large (562) set of images with the Semantic NeRF method which is similar to our network without uncertainty estimations on the *room_1* scene. Our method have showed the best metric values for both predicting semantic labels and predicting color.

Network	mIoU	LPIPS	Avg Acc	Total Acc
Semantic NeRF	0.9313	0.2119	0.9526	0.9903
uSF (both uncertainties)	0.955	0.0757	0.975	0.996
uSF (rgb uncertainty)	0.958	0.0726	0.9727	0.9977
uSF (semantic uncertainty)	0.959	0.0731	0.976	0.9977

TAB. 4. Quality of the semantic 3D-scene reconstruction of uSF and Semantic NeRF methods.

5 Conclusion

In this paper, we have presented a method for reconstructing the neural semantic field along with neural radiance field, which also provides the corresponding uncertainty for both color and semantic labels predictions. Under conditions of a limited number of images in the training set, the model estimating uncertainty shows better reconstruction results compared to the standard model without confidence associated with the predictions. It has been possible to increase the speed of the method by using a special positional encoding method.

As directions for the development of our method, we see the implementation of epistemic uncertainty quantification for semantic labels prediction. We also want to develop the idea of using active learning for segmentation tasks.

FUNDING

This work was supported by Russian Science Foundation, grant No. 20-71-10116, <https://rscf.ru/en/project/20-71-10116/>.

ETHICS APPROVAL AND CONSENT TO PARTICIPATE

This work does not contain any studies involving human and animal subjects

CONFLICT OF INTEREST

The authors of this work declare that they have no conflicts of interest.

References

1. Ben Mildenhall, Pratul P Srinivasan, Matthew Tancik, Jonathan T Barron, Ravi Ramamoorthi, and Ren Ng. Nerf: Representing scenes as neural radiance fields for view synthesis. *Communications of the ACM*, 65(1):99–106, 2021.
2. Yi Wei, Shaohui Liu, Yongming Rao, Wang Zhao, Jiwen Lu, and Jie Zhou. Nerfingmvs: Guided optimization of neural radiance fields for indoor multi-view stereo. In *Proceedings of the IEEE/CVF International Conference on Computer Vision*, pages 5610–5619, 2021.
3. Shuaifeng Zhi, Tristan Laidlow, Stefan Leutenegger, and Andrew J Davison. In-place scene labelling and understanding with implicit scene representation. In *Proceedings of the IEEE/CVF International Conference on Computer Vision*, pages 15838–15847, 2021.

4. Fangfu Liu, Chubin Zhang, Yu Zheng, and Yueqi Duan. Semantic ray: Learning a generalizable semantic field with cross-reprojection attention. In *Proceedings of the IEEE/CVF Conference on Computer Vision and Pattern Recognition*, pages 17386–17396, 2023.
5. Benran Hu, Junkai Huang, Yichen Liu, Yu-Wing Tai, and Chi-Keung Tang. Nerf-rpn: A general framework for object detection in nerfs. In *Proceedings of the IEEE/CVF Conference on Computer Vision and Pattern Recognition*, pages 23528–23538, 2023.
6. Thomas Müller, Alex Evans, Christoph Schied, and Alexander Keller. Instant neural graphics primitives with a multiresolution hash encoding. *ACM Transactions on Graphics (ToG)*, 41(4):1–15, 2022.
7. Peng Wang, Yuan Liu, Zhaoxi Chen, Lingjie Liu, Ziwei Liu, Taku Komura, Christian Theobalt, and Wenping Wang. F2-nerf: Fast neural radiance field training with free camera trajectories. In *Proceedings of the IEEE/CVF Conference on Computer Vision and Pattern Recognition*, pages 4150–4159, 2023.
8. Xuran Pan, Zihang Lai, Shiji Song, and Gao Huang. Activenerf: Learning where to see with uncertainty estimation. In *Computer Vision–ECCV 2022: 17th European Conference, Tel Aviv, Israel, October 23–27, 2022, Proceedings, Part XXXIII*, pages 230–246. Springer, 2022.
9. Kangle Deng, Andrew Liu, Jun-Yan Zhu, and Deva Ramanan. Depth-supervised nerf: Fewer views and faster training for free. In *Proceedings of the IEEE/CVF Conference on Computer Vision and Pattern Recognition*, pages 12882–12891, 2022.
10. Eugen Šlapak, Enric Pardo, Matúš Dopiriak, Taras Maksymyuk, and Juraj Gazda. Neural radiance fields in the industrial and robotics domain: applications, research opportunities and use cases. *arXiv preprint arXiv:2308.07118*, 2023.
11. Carl-Johan Hoel, Krister Wolff, and Leo Laine. Ensemble quantile networks: Uncertainty-aware reinforcement learning with applications in autonomous driving. *IEEE Transactions on Intelligent Transportation Systems*, 2023.
12. Qusay Sellat and Kanagachidambaresan Ramasubramanian. Advanced techniques for perception and localization in autonomous driving systems: A survey. *Optical Memory and Neural Networks*, 31(2):123–144, 2022.
13. Ricardo Martin-Brualla, Noha Radwan, Mehdi SM Sajjadi, Jonathan T Barron, Alexey Dosovitskiy, and Daniel Duckworth. Nerf in the wild: Neural radiance fields for unconstrained photo collections. In *Proceedings of the IEEE/CVF Conference on Computer Vision and Pattern Recognition*, pages 7210–7219, 2021.
14. Jianxiong Shen, Adria Ruiz, Antonio Agudo, and Francesc Moreno-Noguer. Stochastic neural radiance fields: Quantifying uncertainty in implicit 3d representations. In *2021 International Conference on 3D Vision (3DV)*, pages 972–981. IEEE, 2021.
15. Jianxiong Shen, Antonio Agudo, Francesc Moreno-Noguer, and Adria Ruiz. Conditional-flow nerf: Accurate 3d modelling with reliable uncertainty quantification. In *Computer Vision–ECCV 2022: 17th European Conference, Tel Aviv, Israel, October 23–27, 2022, Proceedings, Part III*, pages 540–557. Springer, 2022.
16. Takuhiro Kaneko. Mimo-nerf: Fast neural rendering with multi-input multi-output neural radiance fields. In *Proceedings of the IEEE/CVF International Conference on Computer Vision*, pages 3273–3283, 2023.

17. Sicheng Li, Hao Li, Yue Wang, Yiyi Liao, and Lu Yu. Steernerf: Accelerating nerf rendering via smooth viewpoint trajectory. In *Proceedings of the IEEE/CVF Conference on Computer Vision and Pattern Recognition*, pages 20701–20711, 2023.
18. Alex Yu, Vickie Ye, Matthew Tancik, and Angjoo Kanazawa. pixelnerf: Neural radiance fields from one or few images. In *Proceedings of the IEEE/CVF Conference on Computer Vision and Pattern Recognition*, pages 4578–4587, 2021.
19. Anpei Chen, Zexiang Xu, Fuqiang Zhao, Xiaoshuai Zhang, Fanbo Xiang, Jingyi Yu, and Hao Su. Mvsnerf: Fast generalizable radiance field reconstruction from multi-view stereo. In *Proceedings of the IEEE/CVF International Conference on Computer Vision*, pages 14124–14133, 2021.
20. Wenjing Bian, Zirui Wang, Kejie Li, Jia-Wang Bian, and Victor Adrian Prisacariu. Nope-nerf: Optimising neural radiance field with no pose prior. In *Proceedings of the IEEE/CVF Conference on Computer Vision and Pattern Recognition*, pages 4160–4169, 2023.
21. Christian Reiser, Rick Szeliski, Dor Verbin, Pratul Srinivasan, Ben Mildenhall, Andreas Geiger, Jon Barron, and Peter Hedman. Merf: Memory-efficient radiance fields for real-time view synthesis in unbounded scenes. *ACM Transactions on Graphics (TOG)*, 42(4):1–12, 2023.
22. Zhiwen Yan, Chen Li, and Gim Hee Lee. Nerf-ds: Neural radiance fields for dynamic specular objects. In *Proceedings of the IEEE/CVF Conference on Computer Vision and Pattern Recognition*, pages 8285–8295, 2023.
23. Albert Pumarola, Enric Corona, Gerard Pons-Moll, and Francesc Moreno-Noguer. D-nerf: Neural radiance fields for dynamic scenes. In *Proceedings of the IEEE/CVF Conference on Computer Vision and Pattern Recognition*, pages 10318–10327, 2021.
24. Zhiwen Fan, Peihao Wang, Xinyu Gong, Yifan Jiang, Dejia Xu, and Zhangyang Wang. Nerf-sos: Any-view self-supervised object segmentation from complex real-world scenes. *arXiv e-prints*, pages arXiv–2209, 2022.
25. Mathilde Caron, Hugo Touvron, Ishan Misra, Hervé Jégou, Julien Mairal, Piotr Bojanowski, and Armand Joulin. Emerging properties in self-supervised vision transformers. In *Proceedings of the International Conference on Computer Vision (ICCV)*, 2021.
26. Suhani Vora, Noha Radwan, Klaus Greff, Henning Meyer, Kyle Genova, Mehdi SM Sajjadi, Etienne Pot, Andrea Tagliasacchi, and Daniel Duckworth. Nesf: Neural semantic fields for generalizable semantic segmentation of 3d scenes. *arXiv preprint arXiv:2111.13260*, 2021.
27. David JC MacKay. Bayesian neural networks and density networks. *Nuclear Instruments and Methods in Physics Research Section A: Accelerators, Spectrometers, Detectors and Associated Equipment*, 354(1):73–80, 1995.
28. Radford M Neal. *Bayesian learning for neural networks*, volume 118. Springer Science & Business Media, 2012.
29. Yarín Gal and Zoubin Ghahramani. Dropout as a bayesian approximation: Representing model uncertainty in deep learning. In *international conference on machine learning*, pages 1050–1059. PMLR, 2016.
30. Alexander Amini, Wilko Schwarting, Ava Soleimany, and Daniela Rus. Deep evidential regression. *Advances in Neural Information Processing Systems*, 33:14927–14937, 2020.
31. Murat Sensoy, Lance Kaplan, and Melih Kandemir. Evidential deep learning to quantify classification uncertainty. *Advances in neural information processing systems*, 31, 2018.

32. Alex Kendall and Yarin Gal. What uncertainties do we need in bayesian deep learning for computer vision? *Advances in neural information processing systems*, 30, 2017.
33. Lily Goli, Cody Reading, Silvia Sellán, Alec Jacobson, and Andrea Tagliasacchi. Bayes' rays: Uncertainty quantification for neural radiance fields. *arXiv preprint arXiv:2309.03185*, 2023.
34. Julian Straub and et al. The Replica dataset: A digital replica of indoor spaces. *arXiv preprint arXiv:1906.05797*, 2019.
35. Dmitry Yudin, Yaroslav Solomentsev, Ruslan Musaev, Aleksei Staroverov, and Aleksandr I. Panov. Hpointloc: Point-based indoor place recognition using synthetic rgb-d images. In Mohammad Tanveer, Sonali Agarwal, Seiichi Ozawa, Asif Ekbal, and Adam Jatowt, editors, *Neural Information Processing*, pages 471–484, Cham, 2023. Springer International Publishing.